Boundary states and non-Abelian Casimir effect in lattice Yang-Mills theory

Maxim N. Chernodub,[1] Vladimir A. Goy,[2] Alexander V. Molochkov,[2] and Alexey S. Tanashkin[2]
[1]*Institut Denis Poisson UMR 7013, Université de Tours, 37200 Tours, France*
[2]*Pacific Quantum Center, Far Eastern Federal University, 690950 Vladivostok, Russia*

(Received 3 March 2023; accepted 10 July 2023; published 27 July 2023)

Using first-principles numerical simulations, we investigate the Casimir effect in zero-temperature SU(3) lattice gauge theory in $3+1$ spacetime dimensions. The Casimir interaction between perfect chromometallic mirrors reveals the presence of a new gluonic state with the mass $m_{\rm gt} = 1.0(1)\sqrt{\sigma} = 0.49(5)$ GeV $= 0.29(3)M_{0^{++}}$, which is substantially lighter than the 0^{++} ground-state glueball. We call this excitation "glueton," interpreting it as a nonperturbative colorless state of gluons bound to their negatively colored images in the chromometallic mirror. The glueton is a gluonic counterpart of a surface electron-hole exciton in semiconductors. We also show that a heavy quark is attracted to the neutral chromometallic mirror, thus supporting the existence of a "quarkiton" (a "quark exciton") colorless state in QCD, which is formed by a single quark with its antiquark image in the chromometallic mirror. Analogies with edge modes in topological insulators and boundary states of fractional vortices in multicomponent condensates are highlighted.

DOI: 10.1103/PhysRevD.108.014515

I. INTRODUCTION

The presence of physical macroscopic objects affects fluctuations of quantum fields in the vacuum around them, while the modified fluctuations, in turn, exert the Casimir-Polder force on these physical objects [1]. The phenomenon, known as the Casimir effect [2], is often interpreted as the experimentally measurable evidence [3–5] of the vacuum energy associated with the "zero-point" quantum fluctuations [6,7]. This interpretation originates from the fact that vacuum fluctuations influence neutral objects, such as perfectly conducting neutral metallic objects, that carry no electric or other charges with their dipole and higher-order moments vanishing. Another interpretation of the Casimir effect in terms of the polarization of electric charges in the plates is given in Ref. [8].

The Casimir energy depends not only on the geometry of the objects, but also on interactions of the quantum fields [6,7]. However, in a phenomenologically relevant case of quantum electrodynamics, a correction to the tree–level Casimir effect due to electron-photon interactions is so tiny that it cannot be observed with the existing experimental technology [9].

Remarkably, in strongly coupled theories, the effects of boundaries are much more pronounced: They not only modify the vacuum forces, but also influence the structure of the vacuum itself. For example, analytical studies of effective models suggest the existence of Casimir-induced phase transitions in fermionic effective field theories [10,11] and the $\mathbb{C}P^{N-1}$ model on a finite interval [12,13]. In addition, first-principles numerical simulations show that boundaries in interacting gauge theories, such as compact electrodynamics [14,15] and Yang-Mills theory in two spatial dimensions [16], affect nonperturbative properties, including mass gap generation and (de)confinement (for a review, see Ref. [17]).

Moreover, bounded systems often possess new degrees of freedom that emerge exclusively due to the presence of boundaries. These boundary states and associated boundary central charges ignite substantial interest in the conformal field theories [18,19]. They also appear in the condensed matter systems as the celebrated edge states in topological insulators [20] that have deep roots in the lattice field theory [21].

In our paper, we aim to uncover new, nonperturbative boundary states in Yang-Mills theory and put a bridge between the two phenomena, the Casimir effect and the edge states in the scope of phenomenologically relevant SU(3) Yang-Mills theory in $3+1$ dimensions. What is the relation between the restructuring of the gluonic vacuum in bounded geometries [16]—related, in particular, to the phenomenologically relevant MIT bag model [22,23]—and possible boundary states in Yang-Mills theory? To this end, we first address the Casimir effect on the lattice.

II. CASIMIR EFFECT FOR GLUONS

A. Non-Abelian Casimir effect in continuum theory

Let us first start from the continuum limit, where the non-Abelian Casimir setup features two perfectly conducting flat chromometallic plates in the (x_1, x_2) plane separated by the distance $R = |l_1 - l_2|$ along the x_3 axis, as is shown in the inset in Fig. 1. For Yang-Mills theory with the action in $(3+1)d$ Minkowski spacetime,

$$S = -\frac{1}{4}\int d^4x F^a_{\mu\nu} F^{a,\mu\nu}, \tag{1}$$

the gauge-invariant Casimir boundary conditions are

$$E^a_{\parallel}(x)|_{x\in S} = B^a_{\perp}(x)|_{x\in S} = 0, \quad a = 1, \ldots, N^2 - 1. \tag{2}$$

They imply that the tangential chromoelectric $E^a_i \equiv F^a_{0i}$ and normal chromomagnetic fields $B^a_i = (1/2)\varepsilon_{ijk}F^{a,jk}$ vanish at the surface S (in our case, S is the set of two planes). Conditions (2) are identical, up to the color index $a = 1, \ldots, N^2 - 1$, to the ones imposed on the Abelian electromagnetic (photon) field at the surface of a perfectly conducting metal (a mirror) in electrodynamics. Thus, Eq. (2) correspond to a chromometallic mirror plate for gluons.

In Minkowski spacetime, the canonical energy-momentum tensor reads as follows:

$$T^{\mu\nu} = F^{\mu\alpha}F^{\nu}{}_{\alpha} - \frac{1}{4}\eta^{\mu\nu}F^{\alpha\beta}F_{\alpha\beta}, \tag{3}$$

where $\eta_{\mu\nu} = \mathrm{diag}(1, -1, -1, -1)$ is the metric. The energy density $\mathcal{E}$ is related to its Euclidean counterpart as

$$\mathcal{E} \equiv T^{00} = \frac{1}{2}(\boldsymbol{B}^2 + \boldsymbol{E}^2) \to T^{44}_E = \frac{1}{2}(\boldsymbol{B}^2_E - \boldsymbol{E}^2_E), \tag{4}$$

where the superscript "E" labels the Euclidean quantities.

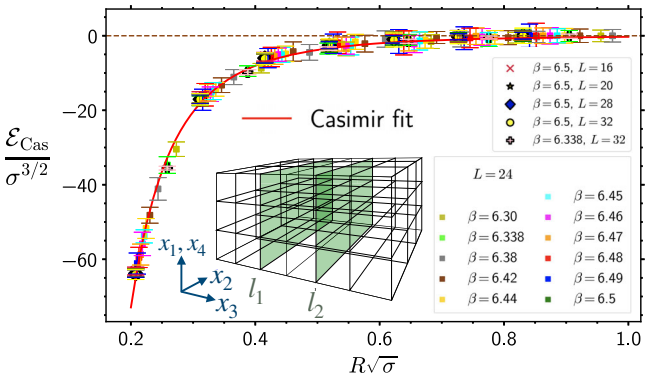

FIG. 1. Casimir energy density $\mathcal{E}_{\mathrm{Cas}}$ vs distance R between the perfect chromometallic plates in units of the fundamental string tension σ for various values of the lattice coupling β and several lattice volumes L^4. The line shows the best fit by the phenomenological function (8), representing the Casimir energy of a massive field. The inset illustrates the Casimir double-plate geometry on the lattice with $R = |l_2 - l_1|$.

B. Casimir effect on the lattice

The formulation of the Casimir problem in lattice gauge theories has been first discussed for Abelian gauge theories in Refs. [24–26] with the extension to the investigation of nonperturbative features of Abelian [14,15] and non-Abelian [16] lattice gauge theories and, more recently, to free fermionic lattice models [27–30]. Below, we will briefly recall the essential points of the construction for gauge theories, referring the interested reader for more details to Ref. [26].

The Wilson form of the lattice Yang-Mills action (1) is given by a sum over lattice plaquettes $P \equiv P_{n,\mu\nu} = \{n, \mu\nu\}$:

$$S = \beta\sum_P (1 - \mathcal{P}_P), \qquad \mathcal{P}_P = \frac{1}{3}\mathrm{ReTr}U_P, \tag{5}$$

where μ and ν label directions, n denotes a site of a $4d$ Euclidean lattice, and $\beta = 6/g^2$ is the lattice coupling. In continuum limit, the lattice spacing vanishes, $a \to 0$, the lattice plaquette $U_{\mu\nu}(n) = U_\mu(n)U_\nu(n+\hat{\mu})U^\dagger_\mu(n+\hat{\nu})U^\dagger_\nu(n) = \exp(ia^2F_{\mu\nu}(n) + \mathcal{O}(a^3))$ reduces to the continuum field-strength tensor $F_{\mu\nu}$, and the lattice action (5) becomes a Euclidean version of Yang-Mills action (1).

The Casimir boundary conditions (2) in the Euclidean lattice formulation are achieved by promoting the lattice coupling in Eq. (5) to a plaquette-dependent quantity $\beta \to \beta_P$, where $\beta_P = \lambda\beta$ if the plaquette P either touches or belongs to the hypersurface spanned by the surface S and $\beta_P = \beta$ otherwise [26]. The quantity λ plays the role of a Lagrange multiplier which, in the limit $\lambda \to \infty$, enforces the lattice version of Eq. (2).

The lattice Casimir energy density per unit area of the Casimir plates on the zero-temperature lattice of the volume L^4_s is given by the properly normalized lattice version of Eq. (4):

$$\mathcal{E}_{\mathrm{Cas}} = \beta L_s\left(\sum_{i=1}^{3}\langle\mathcal{P}_{i4}\rangle_S - \sum_{i<j=1}^{3}\langle\mathcal{P}_{ij}\rangle_S\right), \tag{6}$$

where average plaquettes are taken over the whole lattice volume. Quantity (6) represents the difference between the vacuum expectation values of temporal and spatial plaquettes in the presence of the mirror plates S. An additive divergent contribution to the expectation values of plaquettes, arising from zero-point ultraviolet fluctuations, cancels exactly in Eq. (6). The Casimir energy density (6) is a finite physical quantity that depends only on the distance R between the mirrors and vanishes in their absence (at $R \to \infty$). The Casimir pressure, given by the spatial

diagonal components of (3), is an anisotropic quantity that can also be computed numerically in finite-size Yang-Mills systems [31].

We perform simulations at zero-temperature L_s^4 lattices of various volumes $L_s = 12, 16, 20, 28, 32$ using 13 values of the gauge coupling varying in the range from $\beta = 5.6924$ to $\beta = 6.5$. The physical scaling of the lattice spacing $a = a(\beta)$ is set via the phenomenological value of the fundamental string tension:

$$\sqrt{\sigma} = 485(6)\ \text{MeV} = [0.407(5)\ \text{fm}]^{-1}, \tag{7}$$

following Ref. [32]. Values of $a\sqrt{\sigma}$ for intermediate β's, which cannot be found in Ref. [32], are obtained from an accurate spline interpolation. To generate and update gauge field configurations, we used the Monte Carlo heat bath algorithm [33,34]. For each point, set by the gauge coupling constant β and the lattice distance between plates R/a, we generated 6×10^5 trajectories. The first 10^5 configurations are omitted to achieve thermalization. Next, we proceed to the numerical calculation of the Casimir energy (6) on the lattice.

C. Non-Abelian Casimir energy and the glueton

Figure 1 shows the Casimir energy density between the chromometallic plates (6) calculated from first principles in SU(3) gauge theory. The data for a broad set of lattice volumes and couplings nicely collapse to a smooth curve, thus demonstrating the absence of substantial finite-size and finite-volume effects.

The Casimir energy takes a large negative value as the interplate separation R diminishes. This behavior points to the attractive nature of the non-Abelian Casimir force expected at short separations, where gluons should experience the asymptotic freedom and the Casimir interactions should reduce to the one of a free massless vector field with a color degeneracy factor.

At large interplate separations R, the Casimir energy expectedly vanishes. In theories with a free massless field, the Casimir energy density per unit plate area drops as an inverse power R^{-3} of the distance R, while in field theories with a mass $m \neq 0$, one expects that the Casimir energy density vanishes exponentially: $\mathcal{E}(R) \sim e^{-2mR}$. The factor 2 implies that the particle has to travel from one mirror plate to another and then get reflected to close the path, thus propagating the distance $2R$ in total. Therefore, it is crucial to determine how rapidly the energy diminishes in the large-R limit, as this behavior should uncover the mass spectrum of excitations in the gluonic vacuum between the chromometallic mirrors.

In $(2+1)$-dimensional confining theories, closely spaced chromometallic boundaries are known to affect the vacuum structure between them [15,35]. In SU(2) Yang-Mills theory, the lowest excitation between the plates corresponds to a "Casimir particle" with a mass substantially lower than the lowest glueball mass in the same theory [16]. The Casimir mass is related to the magnetic mass in $2+1$-dimensional Yang-Mills theory [36].

The nonperturbative Casimir energy in $(2+1)d$ non-Abelian gauge theory can successfully be described as the Casimir energy of a massive scalar particle [36]. Applying the same idea in $(3+1)$ dimensions, we fit our numerical results with the Casimir energy of a scalar field [37–39] with certain mass m_{gt}:

$$\mathcal{E}_{\text{Cas}} = -C_0 \frac{2(N_c^2-1)m_{\text{gt}}^2}{8\pi^2 R} \sum_{n=1}^{\infty} \frac{K_2(2nm_{\text{gt}}R)}{n^2}. \tag{8}$$

The prefactor takes into account the (N_c^2-1)-fold color degeneracy (with $N_c = 3$ in our case) as well as two-spin polarization of (massless) gluons. The mass gap could affect this factor, thus forcing us to include a phenomenological parameter C_0. The sum in Eq. (8) is performed over a quickly converging series of modified Bessel functions of the second kind $K_2(x)$.

The best fit of the Casimir energy by function (8) is shown in Fig. 1 by the red line. The fit (with $\chi^2/\text{d.o.f.} \simeq 0.6$ highlighting its good quality) provides us with the following best-fit parameters: $C_0 = 5.60(7)$ and

$$m_{\text{gt}} = 1.0(1)\sqrt{\sigma} = 0.49(5)\ \text{GeV}. \tag{9}$$

Strikingly, the mass of the exchange particle (9) is substantially smaller than the mass of the ground-state glueball $M_{0^{++}} = 3.405(21)\sqrt{\sigma} = 1.653(26)$ GeV [32]. Moreover, the result (9) is surprising, because the ground-state glueball mass $M_{0^{++}}$, by its very definition, is identified with the lowest possible mass in the system. The same phenomenon has been found for an effective particle that governs the long-distance limit of the Casimir effect in two spatial dimensions [16]. Nevertheless, we found an excitation with the nonzero mass (9), which is substantially lower than the lowest ground-state mass.

The apparent contradiction is resolved by noticing that the ground-state glueball mass $M_{0^{++}}$ determines the mass gap in *the bulk* of the system (far from eventual boundaries) while the mass (9) is associated with a new excitation in Yang-Mills theory that emerges exclusively due to the presence of *a boundary*. We call this boundary state "glueton," interpreting it as a nonperturbative colorless state of gluons bound to their negatively colored images in the chromometallic mirror.

The states localized at the boundaries of a system (often called the edge states) can have lower masses than the mass gap in the bulk of the same system. In the condensed matter context, this effect appears at the contacts of semiconductor structures (the Volkov-Pankratov states [40]) and the boundaries of topological insulators (massless edge modes featuring the spin Hall effect [41,42]). However, contrary to

the mentioned boundary modes, the glueton has a nontopological origin.

The glueton is a non-Abelian analog of a surface exciton that emerges in electronic systems. The surface exciton is an electrically neutral quasiparticle that exists in semiconductors and insulators close to their boundaries: An electron (or a hole) in the bulk of the material couples to its image hole (electron) state in the reflective boundary and forms a neutral quasiparticle [43]. These electron-hole states can move only along the boundary of the material. The physics of surface excitons constitutes a vast area of research in solid-state physics [44–47].

The mass of the glueton (9) is of the same order as an effective mass of a gluon which governs an infrared behavior of a gauge-fixed gluon propagator in some approaches to SU(3) gauge theory (see, for example, the recent work in Ref. [48]). There are, however, three reasons why the gluon is different from the glueton.

(i) Contrary to the gluon, the glueton is a colorless object which shares this similarity with a glueball.
(ii) Likewise, the gluon mass is obtained from the gauge-dependent propagator, which requires a gauge fixing, while the Casimir interactions are formulated in the explicitly gauge-invariant way.
(iii) Finally, in the interacting theory, such as Yang-Mills theory, the Casimir energy cannot be expressed via a two-point function, such as the gluon propagator.[1] Thus, the glueton mass and gluon mass, which describe the infrared behavior of these different quantities, are not *a priori* related.

The glueton should also be distinguished from another gluonic excitation, the so-called "gluelump" [49–52]. The gluelump is a purely gluonic system consisting of a valence gluon connected by an adjoint string to a static adjoint source which can be associated with an infinitely heavy gluon. Although the gluelump is not a physical object that cannot be directly measured in an experiment, its theoretical investigation provides valuable insight into the nonperturbative confining properties of QCD [53]. Furthermore, contrary to the gluelump, the glueton can propagate along a reflective domain wall in QCD (for example, along the vacuum-hadronic interface in an MIT bag model [22,23]) and, thus, can potentially contribute to the stability of such states and associated physically measurable quantities.

For completeness of our description, we also mention that Yang-Mills theory possesses yet another, "torelon," excitation which appears in systems with a compact spatial dimension [54]. The torelon corresponds to a confining flux tube that winds around a spatial torus and has no fixed color sources. It has a numerically calculable spectrum corresponding to the eigenstates of the stretched confining string, which cannot collapse due to geometrical topological reasons [55,56]. Recently, it has been revealed that the ground state of the torelon corresponds to an axion-type excitation on the world sheet of the closed flux tube [56,57].

The glueton (a surface state) is yet another gluonic excitation in addition to the glueball (a bulk state), the gluelump (a heavy-light gluon-bound state), and the torelon (a stretched-string state).

III. QUARKS AND MIRRORS

A. The quarkiton: A quark bound by a mirror

We argued above that the chromometallic Casimir plate, acting as a mirror for gluons, facilitates the creation of a colorless (glueton) state bound of gluons to their mirror images. One can question whether a quark can form a colorless bound state with its negative image in a chromometallic mirror, a "quarkiton."

This "quark-chromometallic mirror" bound state is expected to be strengthened by the color confinement phenomenon. Indeed, in the bulk of the confinement phase, the chromoelectric field of a quark is squeezed into the confining string, which terminates, in a meson, on an antiquark. If we place a quark near the non-Abelian mirror, the confining string should terminate on the mirror, thus attracting the quark to its negative image. Therefore, we expect to observe the confinement of a quark with a neutral chromometallic mirror via the formation of the confining QCD string.

Since the mirror is a globally color-neutral object, the induced color charge, which mimics the image antiquark at the mirror, should lead to a redistribution of the color charge over the surface of an (infinite) mirror. In a confining system, the redistributed charge can contribute positively to the total free energy of the quark-mirror system, and it can, in principle, outweigh the negative contribution of the quarkiton bound state.

As we study a purely gluonic system, we cannot investigate the formation of the quarkiton state by calculating the mass spectrum with quark degrees of freedom near the mirror. However, we can calculate the free energy $F_{Q|}(d)$ of a heavy quark "Q" located at the distance d near the mirror "|." This quantity, which has a meaning of a (color-averaged) potential produced by the mirror on the quark, allows us to estimate whether (and how strongly) the quark is attracted to (or repelled by) the mirror.

Associating the potential of the static quark with its free energy $F_{Q|}(d)$, we use the Polyakov loop operator, which places a static heavy quark at the spatial point $\boldsymbol{x}$:

$$P_{\boldsymbol{x}} = \frac{1}{3}\mathrm{ReTr}\left(\prod_{x_4=0}^{L_t-1} U_{\boldsymbol{x},x_4}\right), \tag{10}$$

where the product over the timelike oriented non-Abelian $U_{\boldsymbol{x},x_4}$ matrices is closed via the periodic boundary

[1]The two-point function can be used to calculate the Casimir energy in free theories [6], though.

conditions. The effect of the boundary mirror is identified via the expectation value of the Polyakov loop:

$$\langle P_{\boldsymbol{x}}\rangle_{|}(d) = \exp\{-L_T F_{Q|}(d)\}, \tag{11}$$

placed at the point $\boldsymbol{x} = (x_1, x_2, d)$ in the presence of a single mirror (with fixed $x_3 = 0$) and averaged over the tangential coordinates x_1 and x_2. In Eq. (11), L_T is the lattice length in the imaginary time direction which also serves as an infrared regulator. At finite temperature T, the length L_T is fixed, $L_T = 1/T$, and the term in the exponent of Eq. (11) reduces to the familiar ratio F/T.

In the thermodynamic limit at zero temperature, $L_T \to \infty$, the Polyakov loop observable vanishes identically, making it practically impossible to calculate the potential (11) of the heavy quark at large L_T. This property is of a kinematic rather than dynamical origin, shared by any (even unconfined) massive particle with a finite free energy $F > 0$. Therefore, to prove *qualitatively* the existence of an attractive interaction between a single quark and the mirror, we consider rather a small lattice with the temporal extension $L_T = 12a$, in which the spatial correlator is limited to a few lattice steps due to finite-volume effects.

The expectation value (10) contains unphysical distance-independent contributions, usually subtracted via a renormalization procedure. Because of the small lattice volume, it is challenging to renormalize the quark-free energy via its short-distance behavior, as it is usually done at finite temperature [58]. We notice, however, that the free energy should flatten at the point $d = 6a$ at the middle of the lattice due to the periodicity of the lattice. The flattening at this point is a β-independent feature, which we use as a renormalization requirement to calculate the renormalized free energy $F^{\rm ren}_{Q|}(d) = F_{Q|}(d,\beta) - F_0(\beta)$ near the mirror. The distance-independent subtraction term in our range of β's is described by remarkably simple linear dependence: $F_0(\beta) = -15.5 + 2.9\beta$.

The renormalized free energy of a heavy quark near the mirror, shown in Fig. 2, exhibits reasonable physical scaling, because the points with different lattice cutoffs $a = a(\beta)$ collapse to the same smooth curve. We observe that the flat mirror attracts the quark along the normal direction, thus supporting the formation of the quarkiton bound state. The flattening of the free energy at larger distances l is due to a finite-volume effect which should disappear at larger volumes. At shorter distances, $F^{\rm ren}_{Q|}(l)$ shows qualitative signs of the expected linear behavior. Since the system resides far from the thermodynamic limit, all conclusions drawn from Fig. 2 should be considered qualitative statements.

B. Quarkiton and color confinement

The color confinement property of the low-temperature (hadronic) phase requires that the asymptotic physical states of QCD must be colorless states of quarks and gluons. It is always concluded that quark confinement implies that an isolated quark possesses infinite free energy and, therefore, cannot exist in the hadronic phase [59].

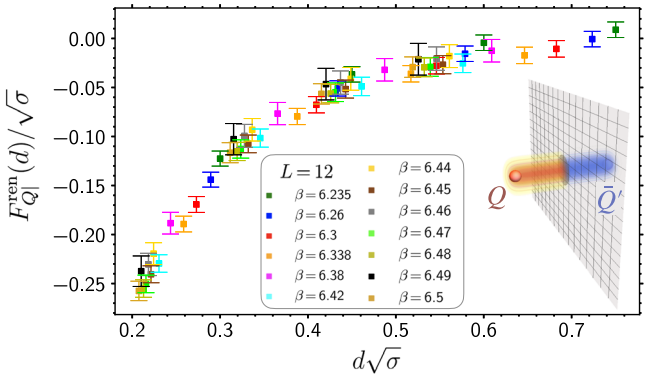

FIG. 2. The renormalized free heavy-quark energy $F^{\rm ren}_{Q|}(d)$ at a distance d from the chromometallic mirror, plotted in physical units, for various lattice coupling constants β at 12^3 lattice. The inset visualizes a quarkiton with the quark Q and its negative image in the chromometallic mirror, the antiquark $\bar{Q}'$, connected by a confining string (the "mirror" part of the string is shown in blue).

Strikingly similar physical properties are shared by fractional vortices in interacting multicomponent Bose-Einstein condensates in two spatial dimensions, as domain walls (strings in $2d$) linearly confine the vortices in bound states that resemble hadrons in QCD [60]. Consequently, an isolated vortex, similarly to an isolated quark, cannot exist in the bulk of the condensate, as a long domain wall attached to the vortex makes its energy infinite. However, single fractional vortices can still survive near the edge of the system, forming a bound state with its boundary (for fractionally charged vortices in superconductors with multiband condensates and the boundary bound states, see Refs. [61–63]).

C. Quarkiton interactions

Our interpretation of the quarkiton boundary states can also be qualitatively supported by investigating the interactions of two quarkitons near the mirror. Let us consider a quark Q and an antiquark $\bar{Q}$ located at the same distance d from the boundary and at a distance l as shown in the inset in Fig. 3. Neglecting the short-distance Coulomb interaction via perturbative gluons, we consider the simplest confining string model, which implies that the energy of a mesonic, quark-antiquark $Q\bar{Q}$ state is $E_1 = \sigma l$. However, if Q and $\bar{Q}$ form quarkiton states with, respectively, their mirror images $\bar{Q}'$ and Q', then the total energy of this system is $E_2 = 2E_{\rm gl} = 2\sigma d$ (we neglect the interaction of the string with the mirror as well as perturbative gluonic exchanges). Therefore, energy arguments suggest that, at short $Q\bar{Q}$ separation $l < 2d$, the common mesonic $Q\bar{Q}$

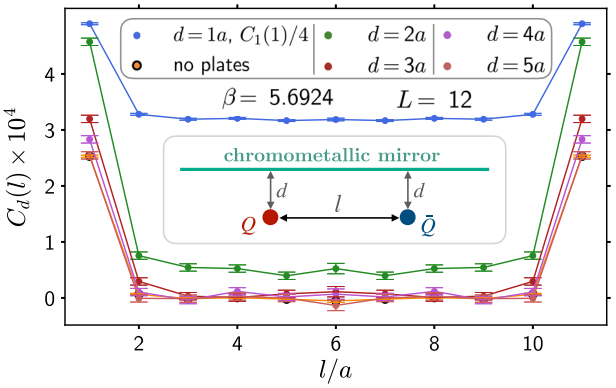

FIG. 3. Correlator of the Polyakov loops $C_d(l)$ for a quark and an antiquark located at the fixed distance d from the chromometallic mirror and separated by the distance l from each other on the lattice 12^4 at $\beta = 5.6924$ ($a\sqrt{\sigma} \simeq 0.4$ [32]). The correlator at $d = 1a$ is scaled by the factor $1/4$. The correlator in the absence of the plates is also shown.

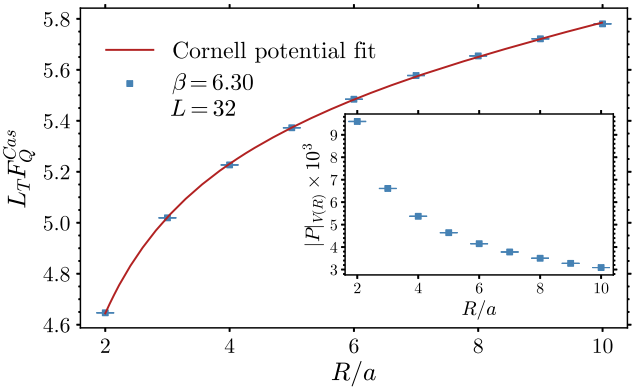

FIG. 4. Mean free energy of a heavy quark in between the mirrors (12) as function of the intermirror separation R/a (in lattice units) on the lattice 32^4. The red line is the best fit by the Cornell potential (13) with the fit parameters $c_1 = 2.03(4)$, $c_2 = 0.044(1)$, and $c_0 = 5.55(2)$. The inset shows the expectation value of the corresponding Polyakov loop (12).

state gets formed. As the separation increases at $l > 2d$, the string rearranges, and the meson decays into two quarkiton states: $Q\bar{Q} \to Q\bar{Q}' + \bar{Q}Q'$.

The string rearrangement can be seen in Fig. 3, although our relatively small ($L = 12$) lattice does not allow us to observe it in detail. At large separation, d from the mirror, $d = 5a$, the correlator of Polyakov loops, $C_d(l) = \langle P(x)P^*(x+l)\rangle_d$ as the function of their mutual distance l, coincides with the same correlator in the absence of the mirrors. Thus, no quarkiton states are formed (a quark attracts to antiquark). As the distance to the mirror diminishes, the correlator increases in magnitude. At a small distance to the mirror d, the correlator reaches the plateaus in l, implying that the free energy of quarks does not depend on their separation l. This physical picture is perfectly consistent with the formation of the quarkiton: The quark and the antiquark attract to their images in the mirror. Moreover, again expectedly, the plateau at $d = 1a$ is higher than at $d = 2a$, in agreement with the fact that the string between the (anti)quark and its image in the mirror is shorter for the quark which is located closer to the mirror. At short distances, the perturbative Coulomb interaction prevails over the string effects [64], but this fact does not change our conclusions given the monotonic nature of the attractive $Q\bar{Q}$ potential.

The boundary (glueton and quarkiton) states can also interact with the bulk (glueball and meson) states. Also, two quarkiton states, confined to the boundary, can combine by producing a colorless meson state which can then propagate into the bulk of the system.

D. A heavy quark between non-Abelian mirrors

Finally, we address the nature of the vacuum between two chromometallic mirrors. In Ref. [16], the same question has been raised in two spatial dimensions for the vacuum of SU(2) gauge theory in between two parallel wires (plates in Euclidean spacetime). It was concluded that, in the confining low-temperature phase, the approaching plates generate a deconfinement phase in the space between them. The deconfinement mechanism in this non-Abelian theory has been related to an identical effect in the $2+1$-dimensional compact Abelian gauge model [35], where the Casimir-induced deconfinement can be explained analytically [65].

We see no pronounced signatures of a phase transition in the space between the plates in the behavior of the non-Abelian Casimir energy (6) shown in Fig. 1. To quantify the effect of the chromometallic mirrors on (de)confining properties of the vacuum, we study another quantity, the unrenormalized free energy of a heavy quark calculated in the space between the plates:

$$L_T F_Q^{\rm Cas}(R) = -\ln|P|_{V(R)} \equiv -\ln\left\langle\left|\sum_{x\in V(R)} P_x\right|\right\rangle, \qquad (12)$$

where the expectation value of the Polyakov loop $|P|_V$ is taken only over the volume $V = V(R)$ between the mirrors separated by the distance R.

In the inset in Fig. 4, we show the Polyakov loop in between the plates $|P|_{V(R)}$. This quantity takes a finite value at small interplate separations R and then quickly diminishes with increasing distance between the plates. Such behavior points to an effective deconfinement regime between the closely spaced plates, which we interpret as a signal of the formation of (a superposition of) finite-energy quarkiton states between the test quark and its antiquark image in the mirrors. As the distance between the plates increases, the free energy of long-stretched quarkiton states rises, and the Polyakov loop vanishes, thus signaling the onset of the confining regime.

The phenomenological interaction between quarks and antiquarks is often described by a Cornell-type potential that combines a linear string behavior at long distances with a short-distance Coulomb interaction [64]. Therefore, the mean free energy of a quarkiton, in which a quark interacts with its antiquark image in the mirror, should follow a similar behavior with the typical quarkiton size set by the interplate separation R. This phenomenological expectation is indeed confirmed in Fig. 4, showing that the free energy (12) is indeed excellently described by the Cornell potential:

$$L_T F_{\mathrm{Q}}^{\mathrm{Cas}}(R/a) = -\frac{c_1}{R/a} + c_2 \frac{R}{a} + c_0, \tag{13}$$

where c_a (with $a = 0, 1, 2$) are the fitting parameters. Equation (13) implies that, at short interplate separations, a heavy quark in the space between the mirrors possesses a finite free energy which we interpret as a deconfinement of color. As the distance between the plates R increases, the free energy increases, leading to the exponential vanishing of the Polyakov loop and the onset of the color confinement.

IV. CONCLUSIONS

Using first-principles numerical simulations, we calculated the nonperturbative non-Abelian Casimir energy generated by two closely spaced chromometallic mirror plates in SU(3) Yang-Mills theory. We also revealed the presence of a new gluonic excitation, the glueton, which we interpret as a colorless bound state of a gluon with its image in a chromometallic mirror.

The glueton is a nontopological excitation that shares similarities with a surface exciton in a superconductor. Unexpectedly, the glueton mass (9) turns out to be lower than the mass of the ground-state 0^{++} glueball. This property of the glueton ("the edge mode is lighter than the mass gap in the bulk") is shared by its topological analogs in condensed matter such as edge modes in topological insulators [20] or the Volkov-Pankratov states at the interfaces of semiconductors [40].

The presence of boundaries also affects the dynamics of quarks. We show that, similarly to confined fractional vortices in multicomponent condensates [60–63], a single isolated quark can exist in the hadronic phase of QCD near (and confined to) a large perfect chromometallic mirror, forming a colorless boundary state: the quarkiton. The glueton and quarkiton states can be relevant near domain walls in QCD and QCD-like theories.

ACKNOWLEDGMENTS

The authors are grateful to Julien Garaud for making them aware about Refs. [61–63]. The numerical simulations were performed at the computing cluster Vostok-1 of Far Eastern Federal University. The work of A. V. M. was supported by Grant No. 0657-2020-0015 of the Ministry of Science and Higher Education of Russia. V. A. G. and A. S. T. have been supported by RSF (Project No. 21-72-00121 [66]) (code development, simulation, and data analysis).

[1] H. B. G. Casimir and D. Polder, The influence of retardation on the London-Van der Waals forces, Phys. Rev. **73**, 360 (1948).
[2] Hendrick B. G. Casimir, On the attraction between two perfectly conducting plates, Proc. K. Ned. Akad. Wet. **51**, 793 (1948).
[3] S. K. Lamoreaux, Demonstration of the Casimir Force in the 0.6 to 6 μm Range, Phys. Rev. Lett. **78**, 5 (1997).
[4] U. Mohideen and Anushree Roy, Precision Measurement of the Casimir Force from 0.1 to 0.9 μm, Phys. Rev. Lett. **81**, 4549 (1998).
[5] G. Bressi, G. Carugno, R. Onofrio, and G. Ruoso, Measurement of the Casimir Force Between Parallel Metallic Surfaces, Phys. Rev. Lett. **88**, 041804 (2002).
[6] K A Milton, *The Casimir Effect* (World Scientific, Singapore, 2001).
[7] Michael Bordag, Galina Leonidovna Klimchitskaya, Umar Mohideen, and Vladimir Mikhaylovich Mostepanenko, *Advances in the Casimir Effect* (Oxford University Press, Oxford, 2009).
[8] R. L. Jaffe, Casimir effect and the quantum vacuum, Phys. Rev. D **72**, 021301 (2005).
[9] M. Bordag, D. Robaschik, and E. Wieczorek, Quantum field theoretic treatment of the Casimir effect, Ann. Phys. (N.Y.) **165**, 192 (1985).
[10] Antonino Flachi, Strongly Interacting Fermions and Phases of the Casimir Effect, Phys. Rev. Lett. **110**, 060401 (2013).
[11] Antonino Flachi, Muneto Nitta, Satoshi Takada, and Ryosuke Yoshii, Sign Flip in the Casimir Force for Interacting Fermion Systems, Phys. Rev. Lett. **119**, 031601 (2017).
[12] Antonino Flachi, Muneto Nitta, Satoshi Takada, and Ryosuke Yoshii, Casimir force for the $\mathbb{C}P^{N-1}$ model, Phys. Lett. B **798**, 134999 (2019).
[13] Alessandro Betti, Stefano Bolognesi, Sven Bjarke Gudnason, Kenichi Konishi, and Keisuke Ohashi, Large-N $\mathbb{CP}^{N-1}$ sigma model on a finite interval and the renormalized string energy, J. High Energy Phys. 01 (2018) 106.
[14] M. N. Chernodub, V. A. Goy, and A. V. Molochkov, Nonperturbative Casimir effect and monopoles: Compact

Abelian gauge theory in two spatial dimensions, Phys. Rev. D **95**, 074511 (2017).
[15] M. N. Chernodub, V. A. Goy, A. V. Molochkov, and A. S. Tanashkin, Casimir boundaries, monopoles, and deconfinement transition in $(3+1)$- dimensional compact electrodynamics, Phys. Rev. D **105**, 114506 (2022).
[16] M. N. Chernodub, V. A. Goy, A. V. Molochkov, and Ha Huu Nguyen, Casimir Effect in Yang-Mills Theory in $D = 2+1$, Phys. Rev. Lett. **121**, 191601 (2018).
[17] M. N. Chernodub, V. A. Goy, and A. V. Molochkov, Nonperturbative Casimir effects in field theories: Aspects of confinement, dynamical mass generation and chiral symmetry breaking, Proc. Sci. Confinement2018 (**2019**) 006.
[18] Christopher P. Herzog and Kuo-Wei Huang, Boundary conformal field theory and a boundary central charge, J. High Energy Phys. 10 (2017) 189.
[19] N. Andrei *et al.*, Boundary and defect CFT: Open problems and applications, J. Phys. A **53**, 453002 (2020).
[20] Markus König, Hartmut Buhmann, Laurens W. Molenkamp, Taylor Hughes, Chao-Xing Liu, Xiao-Liang Qi, and Shou-Cheng Zhang, The quantum spin Hall effect: Theory and experiment, J. Phys. Soc. Jpn. **77**, 031007 (2008).
[21] David B. Kaplan, A method for simulating chiral fermions on the lattice, Phys. Lett. B **288**, 342 (1992).
[22] A. Chodos, R. L. Jaffe, K. Johnson, Charles B. Thorn, and V. F. Weisskopf, A new extended model of hadrons, Phys. Rev. D **9**, 3471 (1974).
[23] A. Chodos, R. L. Jaffe, K. Johnson, and Charles B. Thorn, Baryon structure in the bag theory, Phys. Rev. D **10**, 2599 (1974).
[24] Oleg Pavlovsky and Maxim Ulybyshev, Casimir energy in the compact QED on the lattice, arXiv:0901.1960.
[25] Oleg Pavlovsky and Maxim Ulybyshev, Casimir energy calculations within the formalism of the noncompact lattice QED, Int. J. Mod. Phys. A **25**, 2457 (2010).
[26] M. N. Chernodub, V. A. Goy, and A. V. Molochkov, Casimir effect on the lattice: U(1) gauge theory in two spatial dimensions, Phys. Rev. D **94**, 094504 (2016).
[27] Tsutomu Ishikawa, Katsumasa Nakayama, and Kei Suzuki, Casimir effect for lattice fermions, Phys. Lett. B **809**, 135713 (2020).
[28] Tsutomu Ishikawa, Katsumasa Nakayama, and Kei Suzuki, Lattice-fermionic Casimir effect and topological insulators, Phys. Rev. Res. **3**, 023201 (2021).
[29] Katsumasa Nakayama and Kei Suzuki, Dirac/Weyl-node-induced oscillating Casimir effect, Phys. Lett. B **843**, 138017 (2023).
[30] Yash V. Mandlecha and Rajiv V. Gavai, Lattice fermionic Casimir effect in a slab bag and universality, Phys. Lett. B **835**, 137558 (2022).
[31] Masakiyo Kitazawa, Sylvain Mogliacci, Isobel Kolbé, and W. A. Horowitz, Anisotropic pressure induced by finite-size effects in SU(3) Yang-Mills theory, Phys. Rev. D **99**, 094507 (2019).
[32] Andreas Athenodorou and Michael Teper, The glueball spectrum of su(3) gauge theory in $3+1$ dimensions, J. High Energy Phys. 11 (2020) 172.
[33] Christof Gattringer and Christian B. Lang, *Quantum Chromodynamics on the Lattice* (Springer, Berlin, 2010), Vol. 788.
[34] Joseph F. Boudreau and Eric S. Swanson, *Applied Computational Physics* (Oxford University Press, New York, 2018).
[35] M. N. Chernodub, V. A. Goy, and A. V. Molochkov, Casimir effect and deconfinement phase transition, Phys. Rev. D **96**, 094507 (2017).
[36] Dimitra Karabali and V. P. Nair, Casimir effect in $(2+1)$-dimensional Yang-Mills theory as a probe of the magnetic mass, Phys. Rev. D **98**, 105009 (2018).
[37] P. Hays, Vacuum fluctuations of a confined massive field in two-dimensions, Ann. Phys. (N.Y.) **121**, 32 (1979).
[38] Jan Ambjorn and Stephen Wolfram, Properties of the vacuum. 1. Mechanical and thermodynamic, Ann. Phys. (N.Y.) **147**, 1 (1983).
[39] M. V. Cougo-Pinto, C. Farina, and A. J. Segui-Santonja, Schwinger's method for the massive Casimir effect, Lett. Math. Phys. **31**, 309 (1994).
[40] B. A. Volkov and O. A. Pankratov, Two-dimensional massless electrons in an inverted contact, Sov. J. Exp. Theor. Phys. Lett. **42**, 178 (1985).
[41] M. Zahid Hasan and Charles L. Kane, Colloquium: Topological insulators, Rev. Mod. Phys. **82**, 3045 (2010).
[42] Xiao-Liang Qi and Shou-Cheng Zhang, Topological insulators and superconductors, Rev. Mod. Phys. **83**, 1057 (2011).
[43] Douglas L. Mills and Vladimir Moiseevich Agranovich, *Surface Polaritons: Electromagnetic Waves at Surfaces and Interfaces* (North-Holland, Amsterdam, 1982).
[44] Gregorio H. Cocoletzi and W. Luis Mochán, Excitons: From excitations at surfaces to confinement in nanostructures, Surf. Sci. Rep. **57**, 1 (2005).
[45] Vladimir M. Agranovich, *Excitations in Organic Solids* (Oxford University Press, Oxford, 2009), Vol. 142.
[46] V. I. Gavrilenko, *Optics of Nanomaterials* (Pan Stanford, Stanford, 2011).
[47] P. J. Dean, B. Fischer, D. C. Herbert, J. Lagois, and P. Y. Yu, *Excitons* (Springer Science & Business, New York, 2012), Vol. 14.
[48] Jan Horak, Friederike Ihssen, Joannis Papavassiliou, Jan M. Pawlowski, Axel Weber, and Christof Wetterich, Gluon condensates and effective gluon mass, SciPost Phys. **13**, 042 (2022).
[49] C. Michael, Adjoint sources in lattice gauge theory, Nucl. Phys. **B259**, 58 (1985).
[50] N. A. Campbell, I. H. Jorysz, and Christopher Michael, The adjoint source potential in SU(3) lattice gauge theory, Phys. Lett. **167B**, 91 (1986).
[51] I. H. Jorysz and Christopher Michael, The field configurations of a static adjoint source in SU(2) lattice gauge theory, Nucl. Phys. **B302**, 448 (1988).
[52] Owe Philipsen and Hartmut Wittig, String breaking in SU(2) Yang Mills theory with adjoint sources, Phys. Lett. B **451**, 146 (1999).
[53] Yu. A. Simonov, Gluelump spectrum in the QCD string model, Nucl. Phys. **B592**, 350 (2001).
[54] B. Lucini and M. Teper, Confining strings in SU(N) gauge theories, Phys. Rev. D **64**, 105019 (2001).

[55] K. J. Juge, J. Kuti, F. Maresca, C. Morningstar, and Mike J. Peardon, Excitations of torelon, Nucl. Phys. B, Proc. Suppl. **129**, 703 (2004).

[56] Andreas Athenodorou and Michael Teper, On the mass of the world-sheet "axion" in $SU(N)$ gauge theories in $3+1$ dimensions, Phys. Lett. B **771**, 408 (2017).

[57] Andreas Athenodorou and Michael Teper, The torelon spectrum and the world-sheet axion, Proc. Sci. LATTICE2021 (**2022**) 103.

[58] O. Kaczmarek, F. Karsch, P. Petreczky, and F. Zantow, Heavy quark anti-quark free energy and the renormalized Polyakov loop, Phys. Lett. B **543**, 41 (2002).

[59] Yu. A. Simonov, Confinement, Phys. Usp. **39**, 313 (1996).

[60] D. T. Son and Misha A. Stephanov, Domain walls in two-component Bose-Einstein condensates, Phys. Rev. A **65**, 063621 (2002).

[61] M. A. Silaev, Stable fractional flux vortices and unconventional magnetic state in two-component superconductors, Phys. Rev. B **83**, 144519 (2011).

[62] Daniel F. Agterberg, Egor Babaev, and Julien Garaud, Microscopic prediction of skyrmion lattice state in clean interface superconductors, Phys. Rev. B **90**, 064509 (2014).

[63] Andrea Maiani, Andrea Benfenati, and Egor Babaev, Vortex nucleation barriers and stable fractional vortices near boundaries in multicomponent superconductors, Phys. Rev. B **105**, 224507 (2022).

[64] Nora Brambilla and Antonio Vairo, Quark confinement and the hadron spectrum, in *Proceedings of the 13th Annual HUGS at CEBAF (HUGS 98)* (1999), pp. 151–220, arXiv: hep-ph/9904330.

[65] Alexander M. Polyakov, Quark confinement and topology of gauge groups, Nucl. Phys. **B120**, 429 (1977).

[66] https://rscf.ru/project/21-72-00121/.